

**Interactions between Polystyrene Nanoparticles and Supported Lipid Bilayers: Impact of Charge and Hydrophobicity Modification by Specific Anions**

Journal:	<i>Environmental Science: Nano</i>
Manuscript ID	EN-ART-01-2019-000055.R1
Article Type:	Paper
Date Submitted by the Author:	06-Mar-2019
Complete List of Authors:	Xia, Zehui; University of Massachusetts Amherst, Civil and Environmental Engineering Woods, April ; University of Saskatchewan, Chemistry Burgess, Ian; University of Saskatchewan, Chemistry Lau, Boris; University of Massachusetts Amherst,

Environmental Significance statement

Nanoparticle-Membrane interactions are a complex interplay of a myriad of factors. Elucidating the relative contributions of these factors and identifying the mechanisms involved is the key for enhancing the performance of nanoparticles (e.g., as carriers for targeted drug delivery) and minimizing their unintended consequences (e.g., cytotoxicity). Using a novel combination of quartz crystal microbalance with dissipation monitoring (QCM-D) and surface-enhanced infrared absorption spectroscopy (SEIRAS), this study for the first time revealed the unique importance of chaotropic anions in exerting their influences in membrane disruption by modifying the charge and hydrophobicity of nanoparticles and/or supported lipid bilayers. Our findings have important implications in working towards a rational design of nanoparticles for better control of their cellular uptake.

1
2
3 **Interactions between Polystyrene Nanoparticles and Supported Lipid Bilayers:**
4
5
6 **Impact of Charge and Hydrophobicity Modification by Specific Anions**
7
8
9

10 Zehui Xia^a, April Woods^b, Ian J. Burgess^b, Boris L. T. Lau^a
11

12
13 *^aDepartment of Civil & Environmental Engineering, University of Massachusetts Amherst, 130*
14 *Natural Resources Road, Amherst, MA 01003, USA*
15

16
17 *^bDepartment of Chemistry, University of Saskatchewan, 110 Science Place, Saskatoon, SK*
18 *S7N5C9, Canada*
19

20
21
22 Correspondence: Boris L. T. Lau
23 E-mail: borislau@umass.edu
24
25
26
27
28
29
30
31
32
33
34
35
36
37
38
39
40
41
42
43
44
45
46
47
48
49
50
51
52
53
54
55
56
57
58
59
60

Abstract

Understanding how surface forces and aqueous ions influence the interactions between nanoparticles (NPs) and supported lipid bilayers (SLB) is central to all disciplines interested in studying the nano-bio interface. A prevailing understanding is that cationic NPs have higher penetrating capability across cell membranes. In contrast, we report in this study that anionic polystyrene NPs are capable of binding and penetrating SLB formed by zwitterionic DOPC when charge and hydrophobicity work in concert with specific anions. The preferential deposition of anionic NPs into the bilayer is rationalized electrostatically by considering the slightly positive charge of DOPC. In addition to charge, NP hydrophobicity played an important role in the subsequent penetration of anionic NPs into SLB. The extent of NP deposition was modulated by chaotropic anions (NO_3^-). This study also demonstrates the promise of using a novel combination of surface sensitive techniques, quartz crystal microbalance with dissipation monitoring (QCM-D) and surface-enhanced infrared absorption spectroscopy (SEIRAS), to extend current understanding of NP-SLB interactions to the molecular scale.

1. Introduction

Identifying the mechanisms of interactions of nanoparticles (NPs) with cell membranes is the key for enhancing the performance of NPs in various applications (e.g., as carriers for targeted drug delivery) and minimizing unintended consequences (e.g., cytotoxicity). The potential environmental hazards of nanomaterials are not only determined by the physicochemical properties of NPs but also on the interactions of these NPs with immediate surrounding environment. As the primary protective barrier for all living organisms, cell membrane is a ubiquitous surface that NPs will encounter in the environment. Understanding NP-membrane interactions is essential to better evaluate the toxicity and bioavailability of nanomaterials. NP-membrane interactions are a complex interplay of a myriad of factors including, but not limited to, NP characteristics (e.g., size,¹ shape,¹ charge²), membrane complexity (e.g., membrane protein content and composition³ and the presence of phase-segregated lipid domains⁴) and solution chemistry (e.g., ionic strength⁵ and ion type⁶). Specific interactions between NPs and cell membrane cannot be easily elucidated by cell culture experiments alone. As such, different membrane models,⁷ model NPs,⁸ and analytical tools⁹⁻¹¹ have been used over recent decades and reviewed at length elsewhere.¹²

Many reports in the literature point to the important (yet controversial) role of surface charge in regulating the cellular uptake of NPs.¹³ Cationic NPs are known to cause more disruption of the membrane and stronger mitochondrial and lysosomal damage than anionic NPs.¹³⁻¹⁶ However, for some NPs, such as polylactic-co-glycolic acid (PLGA NPs), charge appears to play no role in cytotoxicity.¹⁷ While Duan and Nie¹⁸ reported preferential cellular uptake of anionic quantum dots, other studies^{19, 20} found greater internalization of cationic quantum dots. Different degrees of NP hydrophobicity may be one reason for these disparate results. Sun et al.²¹ showed that an increase in NP hydrophobicity enhanced the affinity of gold NPs to the cell membrane and induced rapid endocytosis. Using coarse-grained molecular dynamics simulations, Su et al.²² found that semi-hydrophobic NPs are most capable of translocating across membranes. Stellacci et al.^{23, 24} found that gold NPs functionalized with ordered hydrophilic and hydrophobic domains can penetrate the cell membrane through passive diffusion. Specific ion effects, in which ions with the same charge show different behavior, are

1
2
3 known to have an impact on membrane structure (e.g., thickness and curvature).²⁵⁻²⁸
4 Kosmotropic (highly solvated) and chaotropic (poorly solvated) ions are expected to modulate
5 NP-supported lipid bilayer (SLB) interactions by binding to the surface of NPs and/or SLB.
6
7
8
9

10 For the deposition of charged NPs on zwitterionic (charge-neutral) lipids, there are also
11 conflicting reports on whether cationic or anionic NPs have preferential deposition. Inconsistent
12 findings still exist, even when comparing studies from different groups that used the same model
13 lipid and NPs. Granick et al.^{29, 30} suggested that anionic NPs would adsorb more strongly than
14 cationic ones because of the geometrical relation between the P⁻-N⁺ dipole of the headgroup in
15 DOPC (1,2-Dioleoyl-sn-glycero-3-phosphocholine, Figure S1) and the charge of the adsorbing
16 NPs. On the other hand, Zimmermann et al.³¹ suggested that cationic NPs preferentially bind at
17 physiological pH because DOPC has an isoelectric point of about 4. They attributed the charging
18 of the distal membrane leaflet to the unsymmetrical adsorption of hydroxide and hydronium ions.
19
20
21
22
23
24
25
26

27 The contradictory observations mentioned above suggest that the roles of charge, ion
28 specificity, and NP hydrophobicity remain unresolved and stress the need for further
29 investigation on their impact on NP-SLB interactions. Polystyrene NPs (60 nm) are used in this
30 study as a convenient and well-established platform to interrogate nano-bio interactions. They
31 have long been exploited in various applications such as biosensing³² and photonics.³³
32 Polystyrene is well known for its low polydispersity and ability to form stable colloids in
33 biological fluids. In addition to its excellent tunability in size and functionalization, polystyrene
34 NPs recently became an emerging concern due to the potential environmental threat they present.
35 A recent review provided an overview of the literature on the emergence of nanoplastic in the
36 environment and possible impact on human health.³⁴ In 2016, around 335 million metric tons of
37 polymers used as plastics were produced worldwide.³⁴ An estimate of 4.8 to 12.7 million tons of
38 mismanaged plastic waste was generated in 192 coastal countries and discarded into the ocean in
39 the year 2010.³⁵ This study sets itself apart by examining the interactions of charged polystyrene
40 NPs with supported zwitterionic DOPC bilayer using a novel combination of quartz crystal
41 microbalance with dissipation monitoring (QCM-D) and surface-enhanced infrared absorption
42 spectroscopy (SEIRAS). While QCM-D quantifies the deposition dynamics of NPs in real-time,
43 SEIRAS provides evidence of NP interactions with different lipid components (hydrophilic head
44
45
46
47
48
49
50
51
52
53
54
55
56
57
58
59
60

1
2
3 and hydrophobic tail) and the associated changes of interfacial water. Overall, we found that the
4 interplay of three effects (electrostatics, NP hydrophobicity and specific ions) provided a
5 concerted effort to facilitate NP-SLB interactions.
6
7
8
9

10 **2. Experimental section**

11 12 13 **2.1 Materials and Solution Chemistry**

14
15
16
17 DOPC dissolved in chloroform was purchased from Avanti Polar Lipids (Alabaster, AL) and
18 used as received. Its molecular structure is shown in Figure S1. Aminated polystyrene
19 nanoparticles (PS-NH₂) and carboxylated polystyrene nanoparticles (PS-COOH) of 60 nm
20 diameters were purchased from Magsphere Inc. (Pasadena, CA). All solutions were prepared
21 with ACS grade chemicals (Fisher scientific) using Milli-Q (Millipore, Billerica, MA) water with
22 a resistivity of 18.2 MΩ cm. Syringe filters of 0.2 μm pore size (Millipore, Billerica, MA) were
23 used to filter buffer solutions and DOPC vesicle suspensions. All experiments were conducted at
24 the pH of 7.5 ± 0.1. Other chemicals utilized in the experiment include Sodium dodecyl sulfate
25 (SDS) and ethanol to clean the QCM-D flow modules.
26
27
28
29
30
31

32 All experiments were conducted at pH 7.5 using 150 mM electrolytes of either NaF or
33 NaNO₃. Either PBS or HEPES was used as pH buffer to adjust the solution pH. All buffers were
34 filtered through 0.2 μm membrane filter before use.
35
36
37
38
39

40 **2.2 Dynamic Light Scattering**

41
42
43 Hydrodynamic diameters (D_H) of DOPC vesicles and NPs were measured by dynamic light
44 scattering (DLS, Zetasizer Nano, Malvern Panalytical Ltd., Worcestershire, UK). A disposable
45 polystyrene 1 cm cuvette (Sarstedt AG&Co., Nümbrecht, Germany) filled with 1 ml aliquot of
46 the sample was placed in the instrument sample holder. Scattering of the incident light (563 nm
47 wavelength) was measured at 173°. The average D_H were calculated approximately by averaging
48 10-15 individual 10 s measurements. All diameter measurements were conducted at 25 °C. At
49 least five measurements were taken for each sample. Zeta (ζ) potential values were estimated
50 from the electrophoretic mobility (EPM) of 1 ml aliquot solution in a folded capillary cell (DTS
51
52
53
54
55
56
57
58
59
60

1
2
3 1061, Malvern Panalytical Ltd., Worcestershire, UK). Nine measurements of ζ -potentials were
4 conducted for each sample.
5
6
7

8 **2.3 Quartz Crystal Microbalance with Dissipation Monitoring**

9

10
11
12 The formation of DOPC SLB on sensor surfaces and subsequent deposition of NPs were detected
13 by a quartz crystal microbalance with dissipation monitoring (QCM-D, Q-Sense E4, Gothenburg,
14 Sweden). Silica sensors (QSX 303, Q-Sense AB, Gothenburg, Sweden) were used as substrates
15 in all experiments. For cleaning, all sensors were soaked in SDS solution overnight, rinsed by
16 Milli-Q, dried under a nitrogen stream and treated with UV/Ozone Procleaner (Bioforce
17 Nanosciences., Salt Lake City, UT) for 30 minutes. The temperature inside the module was
18 maintained at 25 °C all time. Typical QCM-D experiments involved passing solutions of DOPC
19 vesicle suspension through the flow module that contained the silica sensor at a velocity of 0.1
20 mL/min using a peristaltic pump (Ismatec, Wertheim, Germany), and changes in resonance
21 frequency (Δf) and dissipation (ΔD) were monitored as the mass deposition and film elasticity
22 properties. With the best signal-to-noise ratio, Δf and ΔD obtained from the 7th overtone of are
23 presented and discussed in this study. Representative Δf and ΔD during the formation of DOPC
24 SLB on the silica sensor was shown in Figure S2. Frequency and dissipation changes after the
25 formation of SLB and subsequent rinse of buffer was used as reference in all QCM-D analysis.
26 Following the SLB formation, 0.1 g/L NP suspension was introduced to the flow module and
27 their interaction with SLB was monitored in real-time. After the experiment, QCM-D flow
28 modules were cleaned by rinsing with Milli-Q water and SDS with all tubing connected as
29 described by Cho et al.³⁶
30
31
32
33
34
35
36
37
38
39
40
41
42
43
44

45 **2.4 Surface Enhanced Infrared Absorption Spectroscopy**

46

47
48 In surface-enhanced infrared absorption spectroscopy (SEIRAS), surface enhancement is
49 achieved by modifying the reflecting surface of an internal reflection prism, such as a Si
50 hemisphere, with a thin metallic layer. The preparation of a gold film on a polished Si
51 hemisphere (Harrick Scientific Products, Inc., Pleasantville, New York) for SEIRAS
52
53
54
55
56
57
58
59
60

1
2
3 measurements is described in the Supporting Information and by Miyake et al³⁷ with procedural
4 variations detailed by Rosendahl et al.³⁸
5
6
7

8 Here we employed a solvent-assisted lipid bilayer (SALB) formation method to form
9 continuous and uniform SLB on gold surfaces.^{39, 40} SALB involves a slow and continuous flow
10 of aqueous buffer into the organic phase containing dissolved lipid in which the solid substrate of
11 interest is immersed. We adapted the procedure outlined by Tabaei et al³⁹ to our SEIRAS
12 spectroelectrochemical cell. Details on the SLB formation can be found in the Supporting
13 Information. After SALB formation, increasing concentrations of NP suspension up to 0.1 g/L
14 were added to the cell, followed by the introduction of increasing concentration of electrolyte
15 solutions to a final 150 mM ionic strength. A SEIRA spectrum after DOPC bilayer formation
16 was used as the reference. Alternatively, SEIRA spectra were calculated using the single beam
17 spectrum prior to the formation of the bilayer and these renditions of the data are shown in the
18 Supporting Information. Downward peaks indicate a decrease in absorption for a given vibration
19 mode, due to either less mass density or a diminishing alignment of the transition dipole
20 perpendicular to the substrate surface. Upward peaks demonstrate the increase of the vibration
21 either in density or alignment.
22
23
24
25
26
27
28
29
30
31
32
33

34 **2.5 Octanol-water partition coefficient measurements**

35
36
37

38 Octanol-water partition coefficients (K_{OW}) of NPs were measured to determine the relative
39 hydrophobicity of the polystyrene NPs. We adapted the shake-flask method described by Xiao et
40 al⁴¹ which was analogous to K_{OW} measurements performed for organic compounds. 10 ml
41 octanol and 10 ml buffer solutions were premixed and shaken at 200 rpm on an orbital shaker
42 overnight before use. 150 μ L of 1 g/L NP solutions were added to the aqueous phase carefully,
43 after which the mixture was shaken for another 24 h at room temperature. The mixture was then
44 allowed to stand and equilibrate for approximately 3 h. The aqueous phase was collected for
45 nanoparticle concentration determination by UV-Vis spectrophotometer. The K_{OW} was
46 calculated by comparing initial NPs concentration and aqueous one. Measurements were
47 performed in triplicate.
48
49
50
51
52
53
54
55
56
57
58
59
60

3. Results and discussion

3.1 Anionic PS-COOH induced SLB disruption

Both QCM-D and SEIRAS confirmed the deposition of PS-COOH onto SLB. The exposure of SLB to PS-COOH resulted in a frequency shift (Δf) of 360 Hz (Figure 1a, blue line) and a dissipation shift (ΔD) of 76×10^{-6} (Figure 1a, red line). This indicated that the deposition of PS-COOH induced a change in SLB structure. Before NP deposition, SLB are compact structures lying close to the sensor surface with an almost unmeasurable ΔD of 0.1×10^{-6} (Figure S2). The deposition of PS-COOH caused the SLB to become structurally less compact. SEIRAS peaks associated with polystyrene ($\sim 1450 \text{ cm}^{-1}$, 1500 cm^{-1} , 3010 cm^{-1}) also verified the deposition of PS-COOH (Figure 2a). SEIRAS provided additional information that is invisible to QCM-D by showing downward absorption changes in the C-H stretch ($\sim 2800\text{-}3050 \text{ cm}^{-1}$, ROI 1 in Figure 2a) as well as C=O region ($\sim 1750 \text{ cm}^{-1}$, ROI 2 in Figure 2a), indicating a loss of CH_2 , CH_3 and C=O groups from the bilayer. Hydrocarbon groups are primarily present in the hydrophobic lipid tail region which make up the interior of SLB, while carbonyl groups are generally considered as part of the hydrophilic lipid heads. These observations suggested that once deposited, PS-COOH were able to penetrate the bilayer and displace the lipid components.

The upward feature of the SEIRAS spectra, at wavenumber $> \sim 3700 \text{ cm}^{-1}$, appeared to be an artifact as its line shape was very broad and extended above 3900 cm^{-1} (ROI 3 in Figure 2a). Inspection of the single beam data (Figure S7) reveals a systematic shift in the energy curve at high frequencies upon the increase in ionic strength. Despite this artifact, it is noteworthy that the peak of negative feature associated with the OH stretch region was shifted to low energy ($\sim 3300 \text{ cm}^{-1}$, ROI 3 in Figure 2a) compared to the corresponding feature in highly isolated water molecules which appears above 3700 cm^{-1} .⁴² The position of the OH stretch peak is highly dependent on the extent of hydrogen bonding in water molecules near metal surfaces.^{42, 43} The apparent preferential loss of heavily hydrogen-bonded water potentially indicated that the water cushion layer supporting the SALB-formed SLB was significantly disrupted after the deposition of PS-COOH.

1
2
3 Together with the QCM-D results, the spectral fingerprints provided by SEIRAS
4 suggested that once deposited onto SLB, anionic PS-COOH were able to not only penetrate into
5 the SLB interior and disrupt the bilayer integrity but also affect the distribution of surrounding
6 interfacial water.
7
8
9

10 11 **3.2 Cationic PS-NH₂ did not penetrate SLB**

12
13
14

15 To determine the role of NP surface charge on NP-SLB interaction, the deposition of cationic
16 PS-NH₂ onto SLB was examined accordingly. The addition of PS-NH₂ resulted in a Δf of -1.0
17 Hz (Figure 1b, blue line) and upward absorption changes in the C-H stretch region in the
18 corresponding SEIRAS spectrum ($\sim 2800\text{-}3000\text{ cm}^{-1}$, ROI 1 in Figure 2b). The structure of SLB
19 was slightly less compact after the introduction of PS-NH₂ with a ΔD of 0.4×10^{-6} (Figure 1b,
20 red line). Both Δf and ΔD were in striking contrast to the deposition of PS-COOH ($\Delta f = -360\text{ Hz}$
21 and $\Delta D = 76 \times 10^{-6}$). About 100 seconds after the addition of PS-NH₂, Δf and ΔD were reversed
22 back to -0.4 Hz and 0.2×10^{-6} without further change after rinsing with buffer, suggesting a
23 minimum mass loss and structural change from the substrate surface. This observation is
24 consistent with the loss of water, as indicated by the downward bands observed in the SEIRAS
25 spectra corresponding to the OH stretch region ($\sim 3500\text{ cm}^{-1}$, ROI 3 in Figure 2b). However,
26 there was no evidence of changes in the bilayer due to a lack of substantial changes in the C=O
27 stretch region ($\sim 1750\text{ cm}^{-1}$, ROI 2 in Figure 2b). It is likely that the deposition of PS-NH₂ only
28 displaced the water bound to the lipid head groups without further SLB penetration.
29
30
31
32
33
34
35
36
37
38
39
40

41 Despite the use of zwitterionic lipids (i.e., DOPC), we found that electrostatic forces can
42 still play a role in the interactions. The slightly positive ζ -potential of DOPC ($6.13 \pm 1.11\text{ mV}$,
43 Table 1) provided evidence of an electrostatically favorable condition for the preferential
44 deposition of PS-COOH. In contrast, NP deposition and membrane disruption was suppressed at
45 a lower ionic strength (10 mM NaF) due to electrostatic repulsion between PS-COOH and SLB
46 (see Figures S4 and S5 and Table S1). A SLB consists of two lipid monolayers, each of which
47 contains a hydrophilic lipid head layer facing the bulk solution and a hydrophobic lipid tail layer
48 shielded from the solvent in the center. It is thus expected that hydrophobic NPs would have
49 more interactions with SLB and subsequently alter their structure, leading to membrane
50
51
52
53
54
55
56
57
58
59
60

1
2
3 disruption. Previous studies found that some hydrophobic NPs could penetrate into the bilayer
4 and some semi-hydrophobic NPs with high surface charge density could alter bilayer packing
5 density to induce membrane defects.^{29, 44-46} In this study, we used the octanol-water distribution
6 coefficient (K_{OW}) as a surrogate measure of NP hydrophobicity. Anionic PS-COOH used in this
7 study appeared to be more hydrophobic, with a K_{OW} that is about 7 times of PS-NH₂ (0.89 vs.
8 0.12, Table 1). Upon deposition onto the bilayer, PS-COOH possessed a stronger affinity with
9 the hydrophobic lipid tails, facilitating the membrane disruption (Figure 3a). In contrast, the less
10 hydrophobic PS-NH₂ appeared to stay at the top of the bilayer and only displaced water bound to
11 the phosphatidyl lipid head groups with minimal membrane disruption (Figure 3b).
12
13
14
15
16
17
18
19

20 **3.3 Specific anions modulated the extent of NP deposition**

21
22
23 In addition to the effects of NP surface charge and hydrophobicity, we attempted to understand
24 the role of specific anions in regulating NP-SLB interactions. In the discussion above, we used
25 NaF as the electrolyte to examine the difference in membrane penetration between cationic PS-
26 NH₂ and anionic PS-COOH. The experiment was repeated using a different electrolyte (NaNO₃)
27 under the same ionic strength of 150 mM. Different ions are known to have various preferences
28 to adsorb onto surfaces, subsequently altering their surface chemistry and hydrophobicity.⁴⁷⁻⁵⁷
29 The relative strength of an anion to drive hydrophobic interactions is given by the Hofmeister
30 series, with a typical order of $H_2PO_4^- > F^- > CH_3COOH^- > Cl^- > NO_3^- > SCN^-$ for selected
31 anions.^{47, 48} Some studies also reported the importance of the Hofmeister series in determining
32 colloidal stabilities and cell membrane physicochemical properties.^{26, 49, 51-56, 58, 59} Depending on
33 their positions on the series, anions are generally categorized as kosmotropic (on the left side of
34 the series, such as F^-) or chaotropic (on the right side of the series, such as NO_3^-), which
35 usually correlates with their hydration behaviors and ability to disturb the hydrogen-bonding
36 structure of water molecules.^{47, 48, 50, 51, 55, 57} Kosmotropic anions are highly solvated ions with
37 strong ability of promoting water structures (structure makers). In contrast, chaotropic anions are
38 poorly solvated, with ability to disrupt hydrogen-bonding structures (structure breakers).^{48, 51, 55}
39
40
41
42
43
44
45
46
47
48
49
50
51
52

53 In the case of anionic PS-COOH, our results indicated that NP hydrophobicity is
54 important in driving membrane disruption. According to the Hofmeister series, a chaotropic
55
56
57
58
59
60

1
2
3 anion (NO_3^-) would have a higher affinity with the PS-COOH than F^- .⁵¹ Upon approaching NP
4 surfaces, nitrate anions are more capable in breaking the hydrogen-bonding structure of the
5 hydration shell bound to PS-COOH and subsequently adsorb onto the NPs, resulting in an
6 increase in hydrophilicity of PS-COOH (Figure 5b, Table 1). It has been reported that chaotropic
7 anions have deeper penetration into the bilayer than kosmotropic anions, which may reduce the
8 hydrophobicity of the bilayer interior in a similar way (Figure 5b).^{52-54, 59} We observed that the
9 Δf and ΔD were more substantial in the presence of F^- (-360 Hz and 76×10^{-6} , Figure 1a) than
10 NO_3^- (-35 Hz and 7.2×10^{-6} , Figure 4a). Hence, the hydrophobic interaction between PS-COOH
11 and lipid bilayers can be substantially weakened by nitrate anions.
12
13
14
15
16
17
18
19
20

21 Since PS-NH₂ used in this study were more hydrophilic, the effects of specific ions were
22 not as pronounced ($\Delta f = -8.2$ Hz in NO_3^- vs. -1.0 Hz in F^- , Figures 1b and 4b). This difference
23 could be due to the interactions between anions and the SLB, especially the lipid headgroups.
24 Chaotropic anions have been reported to have higher binding affinity with neutral POPC lipid
25 headgroups than non-chaotropic anions.^{52, 59} Therefore, a greater amount of hydrogen-bonding
26 structure bound to the lipid headgroups would be destroyed in the presence of NO_3^- than F^- ,
27 resulting in a higher loss of SLB interfacial water and subsequently more deposition of PS-NH₂
28 (Figure 6).
29
30
31
32
33
34
35

36 4. Conclusions

37
38
39
40 This study provided insights into the complex nature of interactions between polystyrene NPs
41 and DOPC SLB by examining the interplay of the effects (electrostatic, hydrophobic and specific
42 anions) involved. We found that NP-SLB interaction is a multi-step process: electrostatics-driven
43 deposition of NPs onto the SLB surface, followed by hydrophobic contact and final embedding
44 of NPs. This is consistent with previous computational studies using atomistic and coarse-
45 grained molecular dynamics simulations.⁶⁰⁻⁶⁴ For the first time, the combined use of QCM-D and
46 SEIRAS allows us to better assess the NP deposition dynamics as well as the associated SLB
47 disruption. While cationic PS-NH₂ had minimal interactions with SLB, anionic PS-COOH had a
48 higher extent of 1) deposition, 2) SLB disruption, and 3) disruption of interfacial water. Our
49 results suggest that specific ions exert their influences by modifying the charge and
50
51
52
53
54
55
56
57
58
59
60

1
2
3 hydrophobicity through preferential sorption onto NPs and/or SLB. Further studies are needed to
4 investigate the role of chaotropic anions with different types of NPs in more environmentally and
5 biologically relevant systems.
6
7
8
9
10
11
12
13
14
15
16
17
18
19
20
21
22
23
24
25
26
27
28
29
30
31
32
33
34
35
36
37
38
39
40
41
42
43
44
45
46
47
48
49
50
51
52
53
54
55
56
57
58
59
60

1
2
3 **Conflicts of interest**
4
5

6 There are no conflicts to declare.
7
8

9
10 **Acknowledgements**
11
12

13 This research was financially supported by the US National Science Foundation (CBET
14 1454443) and Natural Science and Engineering Research Council (NSERC) of Canada. The
15 authors would like to thank Dr. Amanda Quirk for her help with the preliminary SEIRAS data
16 collection and valuable discussion.
17
18
19
20
21
22
23
24
25
26
27
28
29
30
31
32
33
34
35
36
37
38
39
40
41
42
43
44
45
46
47
48
49
50
51
52
53
54
55
56
57
58
59
60

References

1. B. D. Chithrani, A. A. Ghazani and W. C. W. Chan, Determining the Size and Shape Dependence of Gold Nanoparticle Uptake into Mammalian Cells, *Nano. Lett.*, 2006, **6**, 662-668.
2. E. Fröhlich, The role of surface charge in cellular uptake and cytotoxicity of medical nanoparticles, *Int. J. Nanomed.*, 2012, **7**, 5577-5591.
3. E. S. Melby, C. Allen, I. U. Foreman-Ortiz, E. R. Caudill, T. R. Kuech, A. M. Vartanian, X. Zhang, C. J. Murphy, R. Hernandez and J. A. Pedersen, Peripheral Membrane Proteins Facilitate Nanoparticle Binding at Lipid Bilayer Interfaces, *Langmuir*, 2018, **34**, 10793-10805.
4. E. S. Melby, A. C. Mensch, S. E. Lohse, D. Hu, G. Orr, C. J. Murphy, R. J. Hamers and J. A. Pedersen, Formation of supported lipid bilayers containing phase-segregated domains and their interaction with gold nanoparticles, *Environ. Sci.: Nano*, 2016, **3**, 45-55.
5. Q. Wang, M. Lim, X. Liu, Z. Wang and K. L. Chen, Influence of Solution Chemistry and Soft Protein Coronas on the Interactions of Silver Nanoparticles with Model Biological Membranes, *Environ. Sci. Technol.*, 2016, **50**, 2301-2309.
6. B. Jing, R. C. T. Abot and Y. Zhu, Semihydrophobic Nanoparticle-Induced Disruption of Supported Lipid Bilayers: Specific Ion Effect, *J. Phys. Chem. B*, 2014, **118**, 13175-13182.
7. Y. F. Dufrêne, W. R. Barger, J.-B. D. Green and G. U. Lee, Nanometer-Scale Surface Properties of Mixed Phospholipid Monolayers and Bilayers, *Langmuir*, 1997, **13**, 4779-4784.
8. C. Loos, T. Syrovets, A. Musyanovych, V. Mailänder, K. Landfester, G. U. Nienhaus and T. Simmet, Functionalized polystyrene nanoparticles as a platform for studying bio-nano interactions, *Beilstein J. Nanotechnol.*, 2014, **5**, 2403-2412.
9. I. Brand, in *Advances in Planar Lipid Bilayers and Liposomes*, eds. A. Iglič and C. V. Kulkarni, Elsevier Academic Press, San Diego, 2013, vol. 18, ch. two, pp. 21-62.
10. L. Wu and X. Jiang, Recent developments in methodology employed to study the interactions between nanomaterials and model lipid membranes, *Anal. Bioanal. Chem.*, 2016, **408**, 2743-2758.
11. J. Schneider, Y. F. Dufrêne, W. R. Barger, Jr. and G. U. Lee, Atomic force microscope image contrast mechanisms on supported lipid bilayers, *Biophys. J.*, 2000, **79**, 1107-1118.
12. A. M. Farnoud and S. Nazemidashtarjandi, Emerging investigator series: interactions of engineered nanomaterials with the cell plasma membrane; what have we learned from membrane models?, *Environ. Sci.: Nano*, 2019, **6**, 13-40.
13. C. M. Goodman, C. D. McCusker, T. Yilmaz and V. M. Rotello, Toxicity of Gold Nanoparticles Functionalized with Cationic and Anionic Side Chains, *Bioconjugate Chem.*, 2004, **15**, 897-900.
14. W. K. Oh, S. Kim, M. Choi, C. Kim, Y. S. Jeong, B. R. Cho, J. S. Hahn and J. Jang, Cellular Uptake, Cytotoxicity, and Innate Immune Response of Silica - Titania Hollow Nanoparticles Based on Size and Surface Functionality, *ACS Nano*, 2010, **4**, 5301-5313.
15. L. Ruizendaal, S. Bhattacharjee, K. Pournazari, M. Rosso-Vasic, L. H. J. de Haan, G. M. Alink, A. T. M. Marcelis and H. Zuilhof, Synthesis and cytotoxicity of silicon

- nanoparticles with covalently attached organic monolayers, *Nanotoxicology*, 2009, **3**, 339-347.
16. A. S. Chauhan, P. V. Diwan, N. K. Jain and D. A. Tomalia, Unexpected In Vivo Anti-Inflammatory Activity Observed for Simple, Surface Functionalized Poly(amidoamine) Dendrimers, *Biomacromolecules*, 2009, **10**, 1195-1202.
17. S. Mura, H. Hillaireau, J. Nicolas, B. Le Droumaguet, C. Gueutin, S. Zanna, N. Tsapis and E. Fattal, Influence of surface charge on the potential toxicity of PLGA nanoparticles towards Calu-3 cells, *Int. J. Nanomed.*, 2011, **6**, 2591-2605.
18. H. Duan and S. Nie, Cell-Penetrating Quantum Dots Based on Multivalent and Endosome-Disrupting Surface Coatings, *J. Am. Chem. Soc.*, 2007, **129**, 3333-3338.
19. J. K. Jaiswal, H. Mattoussi, J. M. Mauro and S. M. Simon, Long-term multiple color imaging of live cells using quantum dot bioconjugates, *Nat. Biotechnol.*, 2002, **21**, 47.
20. X. Zhang and S. Yang, Nonspecific Adsorption of Charged Quantum Dots on Supported Zwitterionic Lipid Bilayers: Real-Time Monitoring by Quartz Crystal Microbalance with Dissipation, *Langmuir*, 2011, **27**, 2528-2535.
21. S. Sun, Y. Huang, C. Zhou, S. Chen, M. Yu, J. Liu and J. Zheng, Effect of Hydrophobicity on Nano-Bio Interactions of Zwitterionic Luminescent Gold Nanoparticles at the Cellular Level, *Bioconjugate Chem.*, 2018, **29**, 1841-1846.
22. C.-F. Su, H. Merlitz, H. Rabbel and J.-U. Sommer, Nanoparticles of Various Degrees of Hydrophobicity Interacting with Lipid Membranes, *J. Phys. Chem. Lett.*, 2017, **8**, 4069-4076.
23. A. Verma, O. Uzun, Y. Hu, Y. Hu, H.-S. Han, N. Watson, S. Chen, D. J. Irvine and F. Stellacci, Surface-structure-regulated cell-membrane penetration by monolayer-protected nanoparticles, *Nat. Mater.*, 2008, **7**, 588.
24. R. C. Van Lehn, P. U. Atukorale, R. P. Carney, Y.-S. Yang, F. Stellacci, D. J. Irvine and A. Alexander-Katz, Effect of Particle Diameter and Surface Composition on the Spontaneous Fusion of Monolayer-Protected Gold Nanoparticles with Lipid Bilayers, *Nano. Lett.*, 2013, **13**, 4060-4067.
25. N. Kucerka, E. Dushanov, K. T. Kholmurodov, J. Katsaras and D. Uhrikova, Calcium and Zinc Differentially Affect the Structure of Lipid Membranes, *Langmuir*, 2017, **33**, 3134-3141.
26. Z. T. Graber, Z. Shi and T. Baumgart, Cations induce shape remodeling of negatively charged phospholipid membranes, *PCCP*, 2017, **19**, 15285-15295.
27. G. Pabst, A. Hodzic, J. Strancar, S. Danner, M. Rappolt and P. Laggner, Rigidification of neutral lipid bilayers in the presence of salts, *Biophys. J.*, 2007, **93**, 2688-2696.
28. A. Catte, M. Girych, M. Javanainen, C. Loison, J. Melcr, M. S. Miettinen, L. Monticelli, J. Määttä, V. S. Oganessian, O. H. S. Ollila, J. Tynkkynen and S. Vilov, Molecular electrometer and binding of cations to phospholipid bilayers, *PCCP*, 2016, **18**, 32560-32569.
29. B. Wang, L. Zhang, S. C. Bae and S. Granick, Nanoparticle-induced surface reconstruction of phospholipid membranes, *Proc. Natl. Acad. Sci. U. S. A.*, 2008, **105**, 18171.
30. Y. Yu, S. M. Anthony, L. Zhang, S. C. Bae and S. Granick, Cationic Nanoparticles Stabilize Zwitterionic Liposomes Better than Anionic Ones, *J. Phys. Chem. C*, 2007, **111**, 8233-8236.

- 1
- 2
- 3
- 4 31. R. Zimmermann, D. Kuttner, L. Renner, M. Kaufmann, J. Zitzmann, M. Muller and C.
- 5 Werner, Charging and structure of zwitterionic supported bilayer lipid membranes
- 6 studied by streaming current measurements, fluorescence microscopy, and attenuated
- 7 total reflection Fourier transform infrared spectroscopy, *Biointerphases*, 2009, **4**, 1-6.
- 8 32. O. D. Velev and E. W. Kaler, In Situ Assembly of Colloidal Particles into Miniaturized
- 9 Biosensors, *Langmuir*, 1999, **15**, 3693-3698.
- 10 33. A. Rogach, A. Susa, F. Caruso, G. Sukhorukov, A. Kornowski, S. Kershaw, H.
- 11 Möhwald, A. Eychmüller and H. Weller, Nano- and Microengineering: 3-D Colloidal
- 12 Photonic Crystals Prepared from Sub- μm -sized Polystyrene Latex Spheres Pre-Coated
- 13 with Luminescent Polyelectrolyte/Nanocrystal Shells, *Adv. Mater.*, 2000, **12**, 333-337.
- 14 34. R. Lehner, C. Weder, A. Petri-Fink and B. Rothen-Rutishauser, Emergence of
- 15 Nanoplastic in the Environment and Possible Impact on Human Health, *Environ. Sci.*
- 16 *Technol.*, 2019, **53**, 1748-1765.
- 17 35. J. R. Jambeck, R. Geyer, C. Wilcox, T. R. Siegler, M. Perryman, A. Andrady, R. Narayan
- 18 and K. L. Law, Plastic waste inputs from land into the ocean, *Science*, 2015, **347**, 768.
- 19 36. N.-J. Cho, C. W. Frank, B. Kasemo and F. Höök, Quartz crystal microbalance with
- 20 dissipation monitoring of supported lipid bilayers on various substrates, *Nat. Protoc.*,
- 21 2010, **5**, 1096.
- 22 37. H. Miyake, S. Ye and M. Osawa, Electroless deposition of gold thin films on silicon for
- 23 surface-enhanced infrared spectroelectrochemistry, *Electrochem. Commun.*, 2002, **4**, 973-
- 24 977.
- 25 38. S. M. Rosendahl, B. R. Danger, J. P. Vivek and I. J. Burgess, Surface Enhanced Infrared
- 26 Absorption Spectroscopy Studies of DMAP Adsorption on Gold Surfaces, *Langmuir*,
- 27 2009, **25**, 2241-2247.
- 28 39. S. R. Tabaei, J.-H. Choi, G. Haw Zan, V. P. Zhdanov and N.-J. Cho, Solvent-Assisted
- 29 Lipid Bilayer Formation on Silicon Dioxide and Gold, *Langmuir*, 2014, **30**, 10363-
- 30 10373.
- 31 40. S. R. Tabaei, J. A. Jackman, S.-O. Kim, V. P. Zhdanov and N.-J. Cho, Solvent-Assisted
- 32 Lipid Self-Assembly at Hydrophilic Surfaces: Factors Influencing the Formation of
- 33 Supported Membranes, *Langmuir*, 2015, **31**, 3125-3134.
- 34 41. Y. Xiao and M. R. Wiesner, Characterization of surface hydrophobicity of engineered
- 35 nanoparticles, *J. Hazard. Mater.*, 2012, **215-216**, 146-151.
- 36 42. K.-i. Ataka, T. Yotsuyanagi and M. Osawa, Potential-Dependent Reorientation of Water
- 37 Molecules at an Electrode/Electrolyte Interface Studied by Surface-Enhanced Infrared
- 38 Absorption Spectroscopy, *J. Phys. Chem.*, 1996, **100**, 10664-10672.
- 39 43. N. Garcia-Araez, P. Rodriguez, H. J. Bakker and M. T. M. Koper, Effect of the Surface
- 40 Structure of Gold Electrodes on the Coadsorption of Water and Anions, *J. Phys. Chem.*
- 41 *C*, 2012, **116**, 4786-4792.
- 42 44. G. Von White, Y. Chen, J. Roder-Hanna, G. D. Bothun and C. L. Kitchens, Structural
- 43 and Thermal Analysis of Lipid Vesicles Encapsulating Hydrophobic Gold Nanoparticles,
- 44 *ACS Nano*, 2012, **6**, 4678-4685.
- 45 45. Y. Li, X. Chen and N. Gu, Computational Investigation of Interaction between
- 46 Nanoparticles and Membranes: Hydrophobic/Hydrophilic Effect, *J. Phys. Chem. B*, 2008,
- 47 **112**, 16647-16653.
- 48 46. B. Jing and Y. Zhu, Disruption of Supported Lipid Bilayers by Semihydrophobic
- 49 Nanoparticles, *J. Am. Chem. Soc.*, 2011, **133**, 10983-10989.
- 50
- 51
- 52
- 53
- 54
- 55
- 56
- 57
- 58
- 59
- 60

- 1
- 2
- 3
- 4 47. F. Hofmeister, Zur Lehre von der Wirkung der Salze, *Naunyn-Schmiedeberg's Arch. Pharmacol.*, 1888, **24**, 14.
- 5
- 6 48. W. Kunz, J. Henle and B. W. Ninham, 'Zur Lehre von der Wirkung der Salze' (about the science of the effect of salts): Franz Hofmeister's historical papers, *Curr. Opin. Colloid Interface Sci.*, 2004, **9**, 19-37.
- 7
- 8
- 9 49. F. Zhang, M. W. A. Skoda, R. M. J. Jacobs, D. G. Dressen, R. A. Martin, C. M. Martin, G. F. Clark, T. Lamkemeyer and F. Schreiber, Gold Nanoparticles Decorated with Oligo(ethylene glycol) Thiols: Enhanced Hofmeister Effects in Colloid-Protein Mixtures, *J. Phys. Chem. C*, 2009, **113**, 4839-4847.
- 10
- 11
- 12
- 13 50. R. Zangi, M. Hagen and B. J. Berne, Effect of Ions on the Hydrophobic Interaction between Two Plates, *J. Am. Chem. Soc.*, 2007, **129**, 4678-4686.
- 14
- 15
- 16 51. C. Calero, J. Faraudo and D. Bastos-González, Interaction of Monovalent Ions with Hydrophobic and Hydrophilic Colloids: Charge Inversion and Ionic Specificity, *J. Am. Chem. Soc.*, 2011, **133**, 15025-15035.
- 17
- 18
- 19 52. R. J. Clarke and C. Lüpfer, Influence of Anions and Cations on the Dipole Potential of Phosphatidylcholine Vesicles: A Basis for the Hofmeister Effect, *Biophys. J.*, 1999, **76**, 2614-2624.
- 20
- 21
- 22
- 23 53. J. J. Garcia-Celma, L. Hatahet, W. Kunz and K. Fendler, Specific Anion and Cation Binding to Lipid Membranes Investigated on a Solid Supported Membrane, *Langmuir*, 2007, **23**, 10074-10080.
- 24
- 25
- 26 54. J. N. Sachs and T. B. Woolf, Understanding the Hofmeister Effect in Interactions between Chaotropic Anions and Lipid Bilayers: Molecular Dynamics Simulations, *J. Am. Chem. Soc.*, 2003, **125**, 8742-8743.
- 27
- 28
- 29
- 30 55. T. López-León, M. J. Santander-Ortega, J. L. Ortega-Vinuesa and D. Bastos-González, Hofmeister Effects in Colloidal Systems: Influence of the Surface Nature, *J. Phys. Chem. C*, 2008, **112**, 16060-16069.
- 31
- 32
- 33 56. T. Oncsik, G. Trefalt, M. Borkovec and I. Szilagyi, Specific Ion Effects on Particle Aggregation Induced by Monovalent Salts within the Hofmeister Series, *Langmuir*, 2015, **31**, 3799-3807.
- 34
- 35
- 36
- 37 57. N. Schwierz, D. Horinek and R. R. Netz, Anionic and Cationic Hofmeister Effects on Hydrophobic and Hydrophilic Surfaces, *Langmuir*, 2013, **29**, 2602-2614.
- 38
- 39 58. N. Kučerka, E. Dushanov, K. T. Kholmurodov, J. Katsaras and D. Uhríková, Calcium and Zinc Differentially Affect the Structure of Lipid Membranes, *Langmuir*, 2017, **33**, 3134-3141.
- 40
- 41
- 42 59. J. R. Rydall and P. M. Macdonald, Investigation of anion binding to neutral lipid membranes using deuterium NMR, *Biochemistry*, 1992, **31**, 1092-1099.
- 43
- 44 60. F. Simonelli, D. Bochicchio, R. Ferrando and G. Rossi, Monolayer-Protected Anionic Au Nanoparticles Walk into Lipid Membranes Step by Step, *J. Phys. Chem. Lett.*, 2015, **6**, 3175-3179.
- 45
- 46
- 47
- 48 61. E. Heikkilä, H. Martinez-Seara, A. A. Gurtovenko, I. Vattulainen and J. Akola, Atomistic simulations of anionic Au₁₄₄(SR)₆₀ nanoparticles interacting with asymmetric model lipid membranes, *Biochimica et Biophysica Acta (BBA) - Biomembranes*, 2014, **1838**, 2852-2860.
- 49
- 50
- 51
- 52 62. R. C. Van Lehn, M. Ricci, P. H. J. Silva, P. Andreozzi, J. Reguera, K. Voitchovsky, F. Stellacci and A. Alexander-Katz, Lipid tail protrusions mediate the insertion of nanoparticles into model cell membranes, *Nature Communications*, 2014, **5**, 4482.
- 53
- 54
- 55
- 56
- 57
- 58
- 59
- 60

- 1
- 2
- 3
- 4 63. R. C. Van Lehn and A. Alexander-Katz, Pathway for insertion of amphiphilic
- 5 nanoparticles into defect-free lipid bilayers from atomistic molecular dynamics
- 6 simulations, *Soft Matter*, 2015, **11**, 3165-3175.
- 7 64. P. Gkeka, P. Angelikopoulos, L. Sarkisov and Z. Cournia, Membrane Partitioning of
- 8 Anionic, Ligand-Coated Nanoparticles Is Accompanied by Ligand Snorkeling, Local
- 9 Disordering, and Cholesterol Depletion, *PLOS Computational Biology*, 2014, **10**,
- 10 e1003917.
- 11
- 12
- 13
- 14
- 15
- 16
- 17
- 18
- 19
- 20
- 21
- 22
- 23
- 24
- 25
- 26
- 27
- 28
- 29
- 30
- 31
- 32
- 33
- 34
- 35
- 36
- 37
- 38
- 39
- 40
- 41
- 42
- 43
- 44
- 45
- 46
- 47
- 48
- 49
- 50
- 51
- 52
- 53
- 54
- 55
- 56
- 57
- 58
- 59
- 60

Figures and Tables

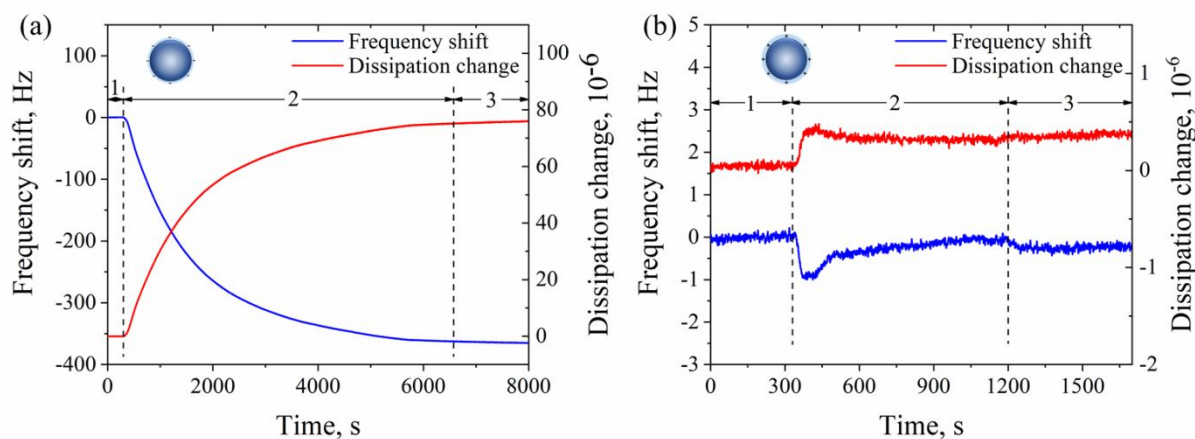


Figure 1. Frequency shifts (blue) and dissipation changes (red) monitored by QCM-D during the deposition of PS-COOH (a) and PS-NH₂ (b) onto SLB at 150 mM NaF, pH 7.5. A typical experiment consists of stages illustrated in the figure: (1) buffer solution only; (2) introduction of NPs; and (3) buffer solution only.

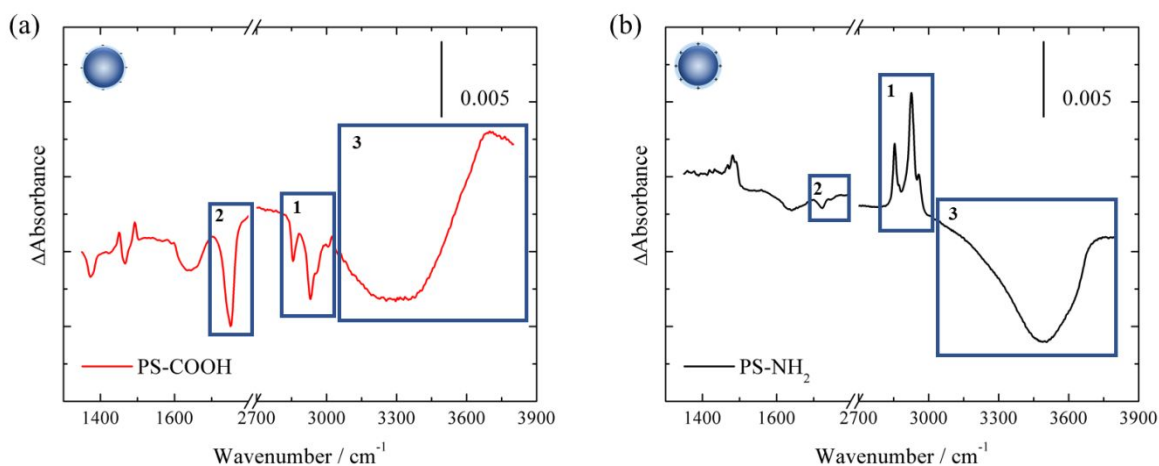


Figure 2. SEIRAS spectra recording the deposition of PS-COOH (a) and PS-NH₂ (b) onto SLB at 150 mM NaF, pH 7.5. The spectra are presented as the change in absorbance referenced to the interface before adding NPs and after the formation of DOPC bilayer. Different regions of interest (ROI) marked as frames in the figure represent: 1) hydrocarbons, 2) carbonyl groups and 3) water regions.

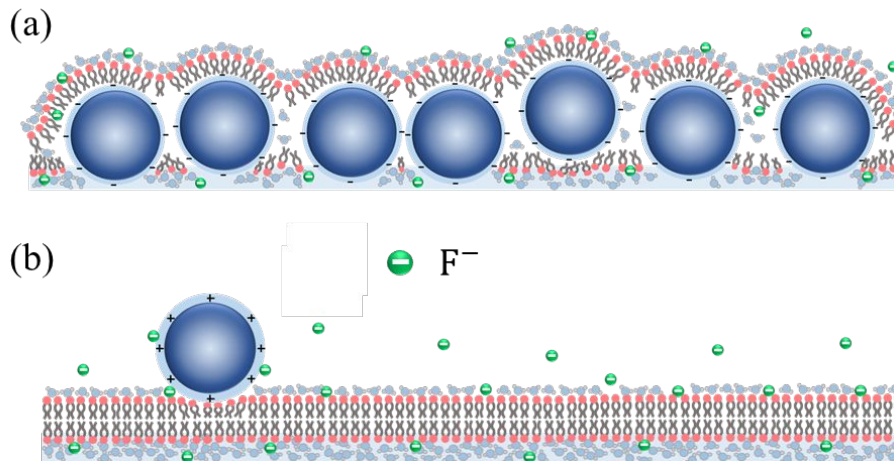


Figure 3. Schematic representations of the interactions of SLB with PS-COOH (a) and PS-NH₂ (b) at 150 mM NaF, pH 7.5 (not drawn to scale).

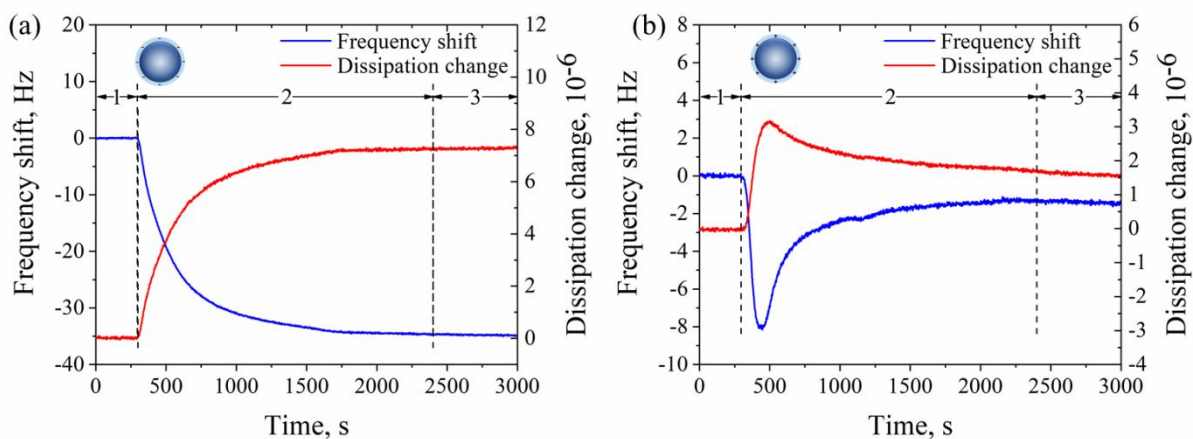
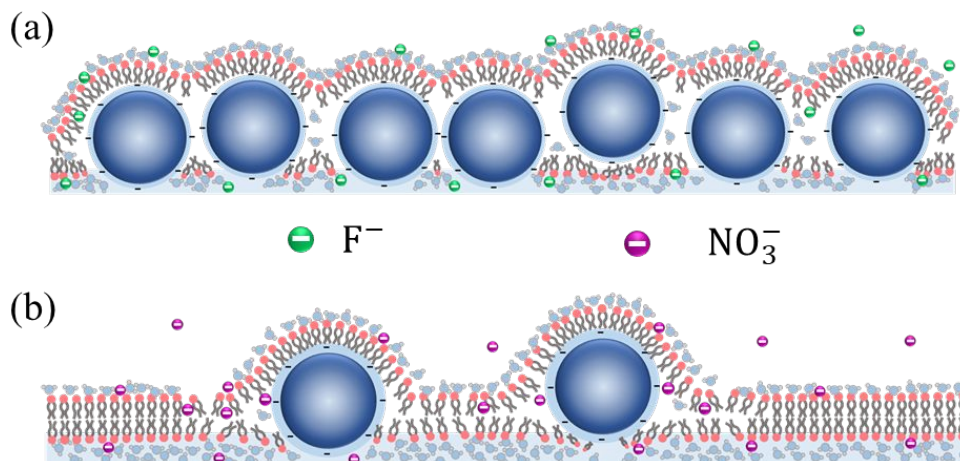
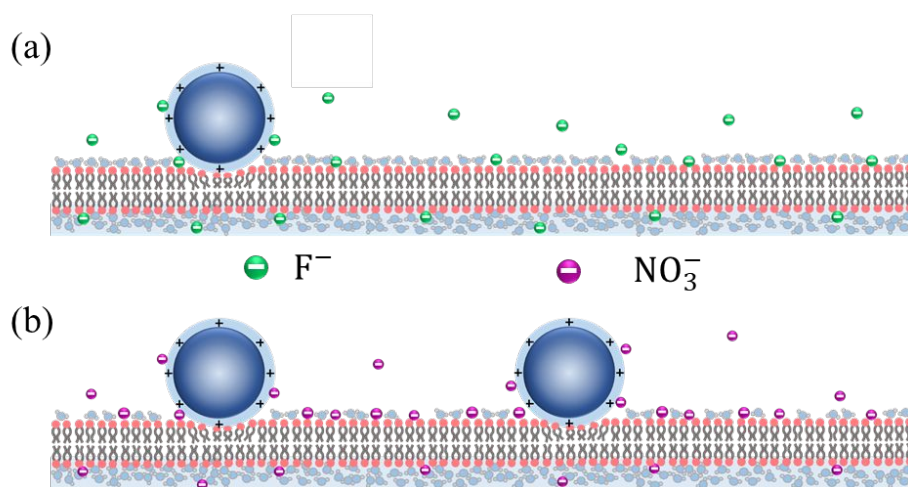


Figure 4. Frequency shifts (blue) and dissipation changes (red) monitored by QCM-D during the deposition of PS-COOH (a) and PS-NH₂ (b) onto SLB at 150 mM NaNO₃, pH 7.5. A typical experiment consists of stages illustrated in the figure: (1) buffer solution only; (2) introduction of NPs; and (3) buffer solution only.



19
20
21
22
23
24
25
26
27
28
29
30
31
32
33
34

Figure 5. Schematic representations of PS-COOH-SLB interactions in the presence of F^- (a) and NO_3^- (b) (not drawn to scale). Note that 1) the hydrophilicity of PS-COOH was enhanced in the presence of NO_3^- , and 2) both PS-COOH and SLB interior possessed greater hydrophilicity since NO_3^- is known for better SLB penetration.



51
52
53
54
55
56
57
58
59
60

Figure 6. Schematic representations of PS-NH₂-SLB interactions in the presence of F^- (a) and NO_3^- (b) (not drawn to scale). Note that there are more NO_3^- adsorbed onto SLB headgroups, which potentially lead to greater interfacial water loss than the scenario with F^- .

Table 1. Physicochemical properties of nanoparticles and lipid vesicles at 150 mM NaF or NaNO₃, pH 7.5.

	D _H , nm		ζ-potentials, mV		K _{ow}	
	NaF	NaNO ₃	NaF	NaNO ₃	NaF	NaNO ₃
PS-COOH	59.29 ± 0.60	56.19 ± 0.60	-41.8 ± 1.63	-41.90 ± 1.96	0.89 ± 0.01	0.39 ± 0.03
PS-NH ₂	60.05 ± 0.75	58.21 ± 0.63	42.2 ± 1.93	35.00 ± 1.58	0.12 ± 0.02	0.23 ± 0.08
DOPC	48.33 ± 0.40	49.15 ± 0.12	6.13 ± 1.11	-5.69 ± 1.35	N/A	N/A